Charge delocalization from cationic substituents into phenanthrene: variation in response among regioisomeric carbocations and carboxonium ions

Kenneth K. Laali * and Sandro Hollenstein

Department of Chemistry, Kent State University, Kent, OH 44242, USA

In an effort to assess charge delocalization and stabilities, a series of regioisomeric PAH–C^+R_2 carbocations (PAH = phenanthrene; R = Me, Ph) were generated from their alcohols by ionization with FSO_3H/SO_2ClF. Model carboxonium ions were also generated by *O*-protonation of the isomeric acetyl- and benzoyl-phenanthrenes with FSO_3H/SO_2ClF. The delocalization paths and the arenium ion character in the resulting carbocations and carboxonium ions are evaluated *via* low temperature NMR studies; conformational aspects in the carboxonium ions are also addressed. The resulting cations may serve as models for epoxide ring opening in biologically active dihydro diols of several classes of PAHs for which the diol epoxide activation path is believed to be significant in cancer induction.

Introduction

A formidable body of experimental evidence points to the PAH diol epoxide activation path as the primary reaction pathway leading to PAH–DNA adduct formation and onset of cell damage in several classes of PAHs.[1–6] Involvement of dihydrotrihydroxy carbenium ions as reactive intermediates in the metabolic activation of PAH–diol epoxides has been established based on numerous solvolytic studies probing the rate, stereochemistry and products.[7–14]

We are engaged in direct studies of PAH carbocations and in charge delocalization mapping at their periphery with the aim of searching for correlations between the mode of charge delocalization and biological activity.[15] In a rather unique way, stable ion chemistry allows the 'bay-region theory' to be experimentally tested.

Along these lines, our recent studies focused on persistent chrysenium and phenanthrenium cations,[16,17] regioisomeric PyC^+R_2 (Py = pyrene) carbocations,[18] and on tuning the electron demand at the carbocation (aryl π-participation) *via* an α-CF_3 in $ArC^+(CF_3)R$ carbocations.[19]

The present study seeks to examine the mode of charge delocalization (as deduced from the magnitude of $\Delta\delta_C$ values)[15,20,21] in a series of phenanthrene-substituted carbocations and their regioisomeric carboxonium ion analogs, in order to gauge the degree of π-participation and arenium ion character depending on the regioisomer. The carbocations and carboxonium ions studied may be viewed as simplified models of dihydro diol ring opening in several classes of PAHs.

Results and discussion

Relationship to carcinogenesis

Chrysene 1,2-dihydro diol **9a** and 3,4-dihydro diol **5a** (Fig. 1) are believed to be the major products of metabolism in rat liver cells whose metabolic activation gives their corresponding *syn*- and *anti*-diol epoxides (**9b/9c** and **5b/5c**).[6] The **5b** isomer has received synthetic attention for biological studies.[1] In the benzo[*a*]anthracene system, the bay-region (1,2) and K-region (5,6) epoxides are biologically most important, but other epoxides including the 8,9-arene oxide **5d** have been synthesized.[22] Synthesis of the triphenylene diol epoxide **7a** has been discussed,[1] but its biological activity has apparantly not been investigated. The bay-region diol epoxide of benzo[*c*]phenanthrene **10a** is highly tumorigenic and has been studied in detail.[5a] Simplifying these structures (Fig. 1) focuses attention on the possible importance of various regioisomeric phenanthrene-substituted carbocations, bearing in mind that these studies merely serve as a guide to *in vivo* reactions where ion pairing and nucleophilic assistance are logically important.

Whereas we have prepared and studied $\mathbf{5}^+$, $\mathbf{6}^+$, $\mathbf{7}^+$ and $\mathbf{8}^+$ (Fig. 2) under stable ion conditions *via* the alcohols **5-OH–8-OH** (Scheme 1), $\mathbf{9}^+$ and $\mathbf{10}^+$ remain elusive since (i) all attempts to

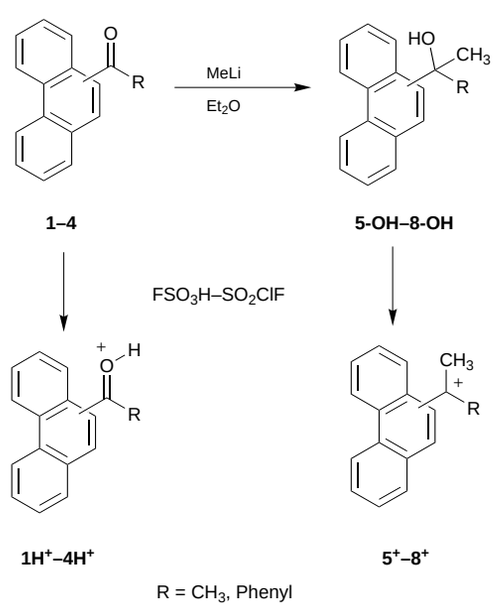

Scheme 1 Synthesis of the isomeric alcohols; generation of carbocations and carboxonium ions

synthesize 1-acetyl- and 1-benzoyl-phenanthrene led to mixtures of 2-, 3- and 9-substituted isomers and (ii) *peri*-strain in the bay-region prevents substitution at C-4 by conventional synthetic means.

For comparison, four examples of persistent carboxonium ions of isomeric acetyl- and benzoyl-phenathrenes $\mathbf{1H}^+$–$\mathbf{4H}^+$ have been provided (Fig. 2).

NMR assignments

Detailed NMR assignments for the α-phenanthrene-substituted carbocations, their alcohol precursors, protonated acetyl- and benzoyl-phenanthrenes and their precursors (Tables 1–4) were

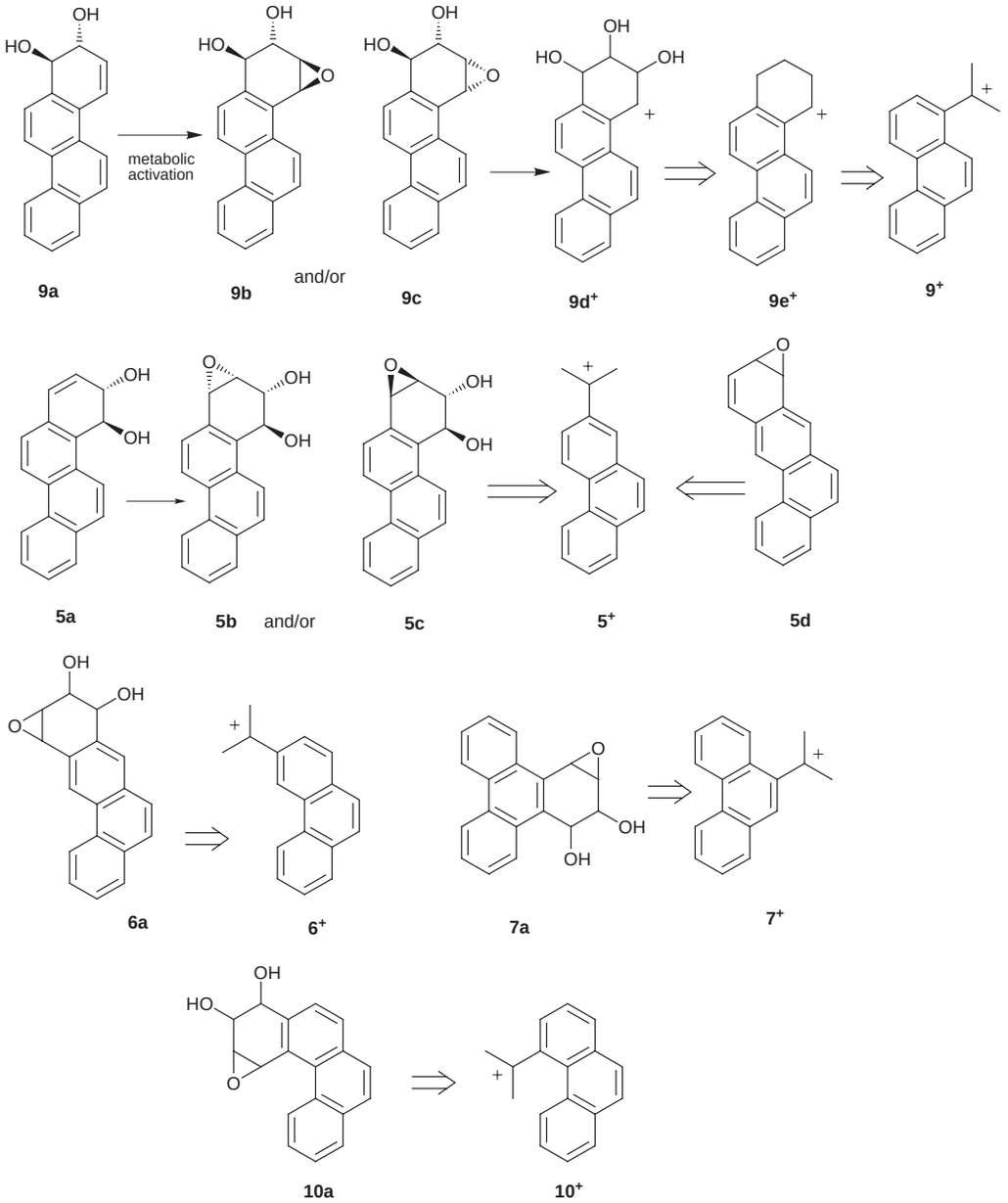

Fig. 1 Analogy between carbocations formed from diol epoxide metabolites and the carbocations generated in this work

based on ^{1}H, ^{13}C, H/H COSY and C/H HETCOR NMR spectra. The low field proton resonances of the bay region (H-4 and H-5, all doublets except H-4 of **2**, **2H**$^{+}$, **6-OH** and **6**$^{+}$) were always the starting point of the assignments, which together with the H/H COSY relationships, allowed the A and C ring protons to be assigned. In the 9-substituted phenanthrenes a very small but significant H/H COSY correlation between H-4 and H-10 was used to determine the A and C ring protons. In some cases a few assignments are still uncertain because of extensive overlap of the resonances.

The ^{13}C NMR resonances of the proton-bearing carbons were assigned with the help of the C/H HETCOR correlations, whereas the quaternary carbons in the neutral compounds were assigned according to the substituent effects and by analogy. In the cations, the calculated charges (AM1) and in particular changes in Mulliken carbon charges $\Delta q = q_c(\text{ion}) - q_c(\text{neutral})$ were used as an additional (*qualitative*) guideline for the assignments;[15–17] the quaternary ^{13}C NMR resonances could not be assigned with certainty. Despite the limitations of semi-empirical methods in predicting charge densities, good correspondence was previously found between the overall pattern of $\Delta\delta_C$ and AM1 charges in a number of PAH carbocations (see refs. 15–17 and related references cited therein). Reasonable qualitative correlations between NMR shifts and calculated (semiempirical) charge densities have also been observed in delocalized polycyclic dianions.[21a,23] Despite their inherent differences, the correspondence between the overall charge pattern derived from *ab initio* and AM1 methods in modelling PAH epoxide ring opening (→carbocation) has been shown.[24]

NMR features of the cations (Tables 1 and 3; Fig. 3)

Carboxonium ions. The C–OH^{+} resonance in **1H**$^{+}$–**4H**$^{+}$ was only observed at temperatures below −45 °C as a very broad singlet at *ca.* δ 13.5. At higher temperatures it broadened further and disappeared into the base line (probably due to fast exchange with the solvent acid).

1H^{+}: A low field singlet at δ 9.03 is characteristic for H-1 and two low field doublets at δ 8.87 and 8.75 for the bay region protons (H-4/H-5) can be observed. In the ^{13}C NMR spectrum, the most deshielded aromatic (observed) resonance is for C-4a (*para* to the acetyl substituent) at δ 42.1.

2H^{+}: The ^{1}H resonance for H-4 appears at very low field (δ 9.89) due to bay region effects and the *ortho* acetyl substituent effect. C-10a (*para* to the substituent) is the most deshielded aromatic resonance (δ 143.6) observed.

3H^{+}: The most deshielded ^{1}H resonances in **3H**$^{+}$ are the H-10

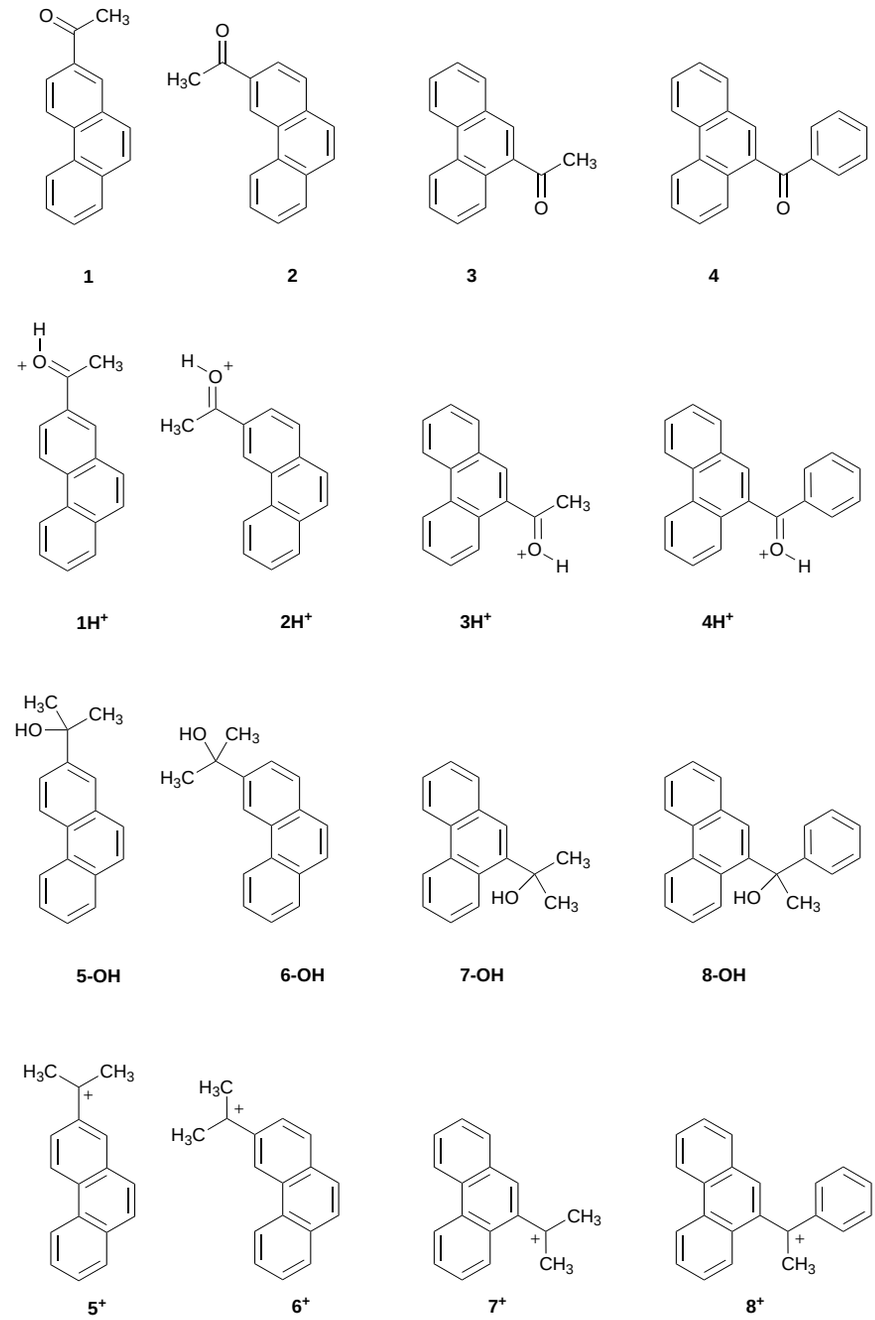

Fig. 2 Regioisomeric acetylphenanthrenes and their carboxonium ions; phenanthrene-substituted alcohols and their carbocations

(singlet at δ 9.32) and the H-8 (doublet at δ 8.95), whereas the bay region protons appear at δ 8.73 and 8.88. The most deshielded ring carbon resonances are the *ortho* carbon *C*-10 (at δ 154.6) and the C4a (at δ 138.7) which is *para* to the protonated acetyl substituent.

4H$^+$: The ^{1}H NMR spectrum of **4H**$^+$ is very complicated due to extensive overlap. The bay region protons (H-4/H-5) are at δ 8.56 and 8.64 and the characteristic singlet for H-10 is at δ 8.16 (see also further discussion).

Carbocations. 5$^+$: The proton resonances are similar to **1H**$^+$ but more deshielded. The H-1 singlet is at δ 9.39 and the bay region protons are at δ 8.93 and 8.87. The most deshielded ring carbon resonance is observed at δ 148.4 and the C$^+$ is at δ 238.5.

6$^+$: The very low field singlet at δ 10.08 was unambigously assigned to the bay region proton which is also *ortho* to the carbocation center. The other bay region proton is observed at δ 8.90. In **6**$^+$, the carbocation center has a chemical shift of δ 234.7 and the most deshielded ring carbon atom is C10a (δ 148.2, *para* to the substituent).

7$^+$: The most deshielded proton resonances for **7**$^+$ are the H-10 (at δ 9.58) and the bay region Hs (at δ 8.77 and 8.82). The most deshielded ring carbon resonances are for C-10 and C-3 (δ 159.6 and 143.2, respectively).

8$^+$: The ^{1}H NMR spectrum of **8**$^+$ is rather complicated due to extensive overlap of the signals. The bay region protons appear at δ 8.78 and 8.93. For this cation the resonance for C$^+$ is at δ 218.9 and the most deshielded aromatic carbon resonance is the C-10 (δ 158.0).

AM1 calculations

AM1 calculated changes in carbon charges $\Delta q = q_{C(ion)} - q_{C(neutral)}$ qualitatively support the overall mode of charge delocalization as deduced based on $\Delta\delta_C$ values. Thus AM1-predicted charge alternation paths are generally the same as those deduced based on NMR experiments, except for C-7 in **3H**$^+$, **4H**$^+$, **7**$^+$ and **8**$^+$, where the calculated charges are much higher than the observed chemical shifts would suggest (see earlier comments on the use of semiempirical methods).

Table 1 ^{1}H NMR data for the carboxonium ions and carbocations

	Chemical shift (ppm)[a]							
H-atom	**1H$^+$**	**2H$^+$**	**3H$^+$**	**4H$^+$**	**5$^+$**	**6$^+$**	**7$^+$**	**8$^+$**
1	9.03	8.16	8.24	7.67–7.83	9.39	7.97	8.42	8.13–8.18
2	—	8.45	7.88	7.67–7.83	—	8.54	7.93*	7.82*
3	8.42	—	8.15	7.94	8.60	—	8.36	8.13–8.18
4	8.87	9.89	8.72	8.56	8.93	10.08	8.77	8.78
5	8.75	8.85	8.80	8.64	8.87	8.90	8.82	8.83
6	7.89	7.93	7.91	7.67–7.83	7.91	8.04	7.99*	7.86–8.00
7	7.85*	7.86	7.91	7.67–7.83	8.07*	7.91	7.99*	7.86–8.00
8	8.02*	8.08	8.95	8.32	8.02*	8.14	8.31	7.86–8.00
9	7.99*	8.26	—	—	8.07*	8.54	—	—
10	7.89*	7.93	9.32	8.16	8.07*	8.16	9.58	8.05
CH_3	3.38	3.45	3.46	—	3.47	3.42	3.46	3.78
					3.50	3.54	3.47	
Ph(*ortho*)	—	—	—	8.10	—	—	—	8.13–8.18
Ph(*meta*)	—	—	—	7.89	—	—	—	7.86–8.00
Ph(*para*)	—	—	—	7.63–7.83	—	—	—	8.32

[a] * = Assignment may be interchanged (within same molecule).

Table 2 ^{1}H NMR data for the precursors

	Chemical shift (ppm)[a]							
H-atom	**1**	**2**	**3**	**4**	**5-OH**	**6-OH**	**7-OH**	**8-OH**
1	8.41	7.90	7.93	7.78	8.00	7.86	7.86	7.98
2	—	8.11	7.63	7.48–7.63	—	7.74	7.59	7.64
3	8.13	—	7.74	7.48–7.63	7.78	—	7.63	7.69
4	8.63	9.28	8.65	8.61	8.65	8.90	8.64	8.67
5	8.62	8.75	8.69	8.65	8.67	8.79	8.75	8.70
6	7.65	7.73	7.68*	7.48–7.63	7.60	7.70*	7.65*	7.50
7	7.65	7.64	7.68*	7.48–7.63	7.66	7.66*	7.65*	~7.3
8	7.88	7.90	8.74	8.05	7.90	7.92	8.93	7.98
9	7.75	7.82*	—	—	7.75	7.74	—	—
10	7.75	7.66*	8.17	7.76	7.75	7.74	7.82	8.15
CH_3	2.75	2.78	2.82	—	1.72	1.76	1.91	2.15
Ph(*ortho*)	—	—	—	7.87	—	—	—	7.46
Ph(*meta*)	—	—	—	7.38	—	—	—	~7.3
Ph(*para*)	—	—	—	~7.5	—	—	—	~7.2

[a] * = Assignment may be interchanged (within same molecule).

Table 3 ^{13}C NMR data for the carboxonium ions and carbocations

	Chemical shift (ppm)[a]							
C-atom	**1H$^+$**	**2H$^+$**	**3H$^+$**	**4H$^+$**	**5$^+$**	**6$^+$**	**7$^+$**	**8$^+$**
1	n.o.	131.8	135.1	129.5*	148.2	127.7	139.1	137.0
2	*b*	n.o.	129.7	128.9*	*c*	132.7	130.1*	130.1*
3	n.o.	*d*	138.7	133.1	132.6	*e*	143.2	139.0
4	126.1	n.o.	124.2	123.4	126.9	141.8	124.3	124.4
4a	142.1	*d*	138.7	148.0	148.4	129.8	*f*	*g*
4b	*b*	*d*	*h*	*i*	*j*	*e*	*k*	*l*
5	125.7	123.3	124.8	124.0	127.6	123.4	125.2	125.1
6	128.0	130.4	130.1	129.5*	129.8	132.4	130.8*	130.5*
7	132.5	129.9	131.2	129.5*	135.8	130.6	130.9*	131.3*
8	130.1*	130.6	127.6	126.2	129.5*	131.8	129.0	129.6*
8a	*b*	*d*	*h*	*i*	*c*	*e*	*f*	*l*
9	131.2*	138.7	*h*	*i*	132.0*	146.5	*k*	*g*
10	129.2*	126.9	154.6	141.7	130.4*	132.6	159.6	158.0
10a	*b*	143.6	*h*	*i*	*j*	148.2	*k*	*l*
COH^+/C^+	216.0	215.3	214.4	207.6	238.5	234.7	230.1	218.9
CH_3	24.8	24.9	26.8	—	31.7	31.3	31.1	—
					32.1	31.9	35.5	
Ph(*ipso*)	—	—	—	*i*	—	—	—	*l*
Ph(*ortho*)	—	—	—	136.3	—	—	—	139.7
Ph(*meta*)	—	—	—	130.6	—	—	—	131.7
Ph(*para*)	—	—	—	134.5	—	—	—	145.3

[a] * = Assignment may be interchanged (within same molecule); n.o. = not observed. [b] 136.4, 131.1, 129.5, n.o. [c] 138.9, 137.4. [d] 133.3, 131.8, 130.5, 129.2. [e] 135.9, 133.1, 132.1. [f] 142.8, 142.3. [g] 145.0, 138.3. [h] 131.3, 129.6, 127.1, 125.2. [i] 135.0, 131.9, 128.8, 127.4, 125.1. [j] 133.0, 129.2. [k] 131.2, 129.6, 127.9. [l] 132.1, 130.3, 130.0, 125.4.

Table 4 ^{13}C NMR data for the precursors

	Chemical shift (ppm)[a]							
C-atom	**1**	**2**	**3**	**4**	**5-OH**	**6-OH**	**7-OH**	**8-OH**
1	129.7	128.8	129.7	129.1	123.6	128.4	128.9	129.5*
2	*b*	125.3	127.0	127.1*	147.3	123.6	126.6*	127.2
3	125.0	*c*	128.9	128.2*	123.7	147.2	126.7*	127.4
4	123.0	123.8	122.6	122.6	122.7	117.6	122.2	122.8
4a	*b*	*c*	*d*	*e*	*f*	*g*	*h*	*i*
4b	*b*	*c*	*d*	*e*	*f*	*g*	*h*	*i*
5	123.2	122.6	122.7	122.9	122.6	122.6	123.2	123.4
6	126.9*	126.2	127.5*	127.1*	126.4	126.6*	125.8*	126.2
7	127.6*	127.1	127.0*	127.1*	126.5	126.4*	125.8*	126.2*
8	128.6*	128.8	126.7	126.5	128.5	128.5	128.1	128.7*
8a	*b*	*c*	*d*	*e*	*f*	*g*	*h*	*i*
9	127.7*	129.6*	134.6	138.1	127.1*	126.4*	141.2	148.5
10	127.2*	127.2*	130.6	129.4	127.0*	126.4*	123.7	125.7
10a	*b*	*c*	*d*	*e*	128.5	*g*	*h*	*i*
C=O	197.8	198.1	201.8	197.8	72.6	72.9	73.9	77.0
CH_3	26.6	26.8	29.9	—	31.8	31.8	31.4	—
Ph(*ipso*)	—	—	—	135.2	—	—	—	140.3
Ph(*ortho*)	—	—	—	130.3	—	—	—	125.5
Ph(*meta*)	—	—	—	128.4	—	—	—	128.8
Ph(*para*)	—	—	—	133.3	—	—	—	127.2*

[a] * = Assignment may be interchanged (within same molecule). [b] 134.7, 133.2, 132.8, 131.2, 129.6. [c] 134.8, 134.7, 132.1, 130.6, 129.7. [d] 131.9, 130.7, 129.8, 128.2. [e] 131.2, 130.5, 130.1, 130.0. [f] 131.9, 131.8, 130.1. [g] 132.1, 130.6, 130.3, 129.8. [h] 131.5, 131.0, 130.1, 129.9. [i] 132.1, 131.3, 130.9, 130.0.

Table 5 Magnitude of carbon deshielding values in carboxonium ions and carbocations

	$\Delta\delta_C$ C=O$^+$H/ C=O (ppm)	$\Sigma\Delta\delta_C$(arom.) (ppm)
1H$^+$	+18.2	*a*
2H$^+$	+17.2	*a*
3H$^+$	+12.6	+51.1
4H$^+$	+9.6	+28.3/+21.0[b]
	$\Delta\delta_C$ C$^+$/ COH	$\Sigma\Delta\delta_C$(arom.) (ppm)
5$^+$	165.9	+79.6
6$^+$	161.8	+82.5
7$^+$	156.2	+91.3
8$^+$	141.9	+54.1/44.1[b]

[a] Not all ^{13}C resonances were observed in the carbocations. [b] Phenanthrene carbons/phenyl carbons.

A comparative discussion of carboxonium ions and the carbocations

The magnitude of charge delocalization into the phenanthrene system is much larger in the carbocations **5$^+$**–**8$^+$** than in the carboxonium ions **1H$^+$**–**4H$^+$**. The ^{13}C chemical shifts of the aromatic carbons of the cations **5$^+$**–**8$^+$** are much more deshielded (*ca.* 40 ppm) as compared to **1H$^+$**–**4H$^+$**, which is in agreement with the oxonium ion character of **1H$^+$**–**4H$^+$**.

The charge alternation path in different substituted phenanthrenes

The charge alternation modes for the 2-, 3- and 9-substituted phenanthrenes are totally diverse. In the 2-substituted cations **1H$^+$** and **5$^+$**, the delocalization path is mainly centered around ring A and C and the most deshielded aromatic carbon is C-4a (*para* to the substituent). In the 3-substituted cations (**2H$^+$** and **6$^+$**), the charge is localized in ring A and B with C-10a being the most deshielded (*para* to the substituent). In the 9-substituted cations the positive charge is mostly localized on the A and B rings, but with C-10 as the most deshielded carbon (*ortho* to the acetyl substituent). In all cases, the protonated ketones show the same delocalization path as the carbocations, but the arenium ion character is significantly lower (smaller $\Delta\delta$s). The comparison between the two pairs of 9-substituted cations **3H$^+$/4H$^+$** and **7$^+$/8$^+$** indicates that the phenyl group reduces phenanthrenium ion character, whereby additional stabilization is gained by delocalization into the phenyl group in **4H$^+$** and **8$^+$** as compared to the methyl groups in **3H$^+$** and **7$^+$**.

Stabilization of the positive charge depending on substitution

If one compares the NMR characteristics of the regioisomeric (2,3,9) α-phenanthrene-substituted carbocations and carboxonium ions with each other, it becomes apparent that the delocalization of the positive charge into the phenanthrene moiety is best in the 9-substituted cases (**3H$^+$**, **4H$^+$**, **7$^+$** and **8$^+$**), followed by the 3-substituted cations (**2H$^+$** and **6$^+$**). Charge delocalization into the phenanthrene moiety *via* the 2-position (as in **1H$^+$** and **5$^+$**) is least effective (see Table 5). Thus the $\Delta\delta_C$ values for the carbonyl carbon in the carboxonium ions decrease from **1H$^+$** to **4H$^+$**, indicative of increased oxonium ion character. The same order is observed in the carbocations **5$^+$**–**8$^+$**, where the $\Delta\delta_C$ values for the C$^+$ center decrease from **5$^+$** to **8$^+$**, showing that carbocation **5$^+$** is least delocalized whereas **8$^+$** is most effectively delocalized. At the same time, the chemical shifts of the aromatic carbons in the 9-substituted phenanthrenes are more deshielded than in the 3-substituted cases, which are in turn more deshielded than the 2-substituted phenanthrenes. The increase in $\Sigma\Delta\delta_C$ values for the aromatic carbons from **1H$^+$** to **4H$^+$** and **5$^+$** to **8$^+$** clearly indicate that the stabilization of the positive charge is most effective in the 9-substituted cations and least effective in the 2-substituted analogs.

Conformational aspects related to rotation around C$^+$–C(*ipso*) and (HO$^+$=C)–C(*ipso*) bonds

Due to the delocalization of the positive charge into the phenanthrene system, the C$^+$–C(*ipso*) and (HO$^+$=C)–C(*ipso*) bonds show significant double bond character. The CH_3 groups in carbocations **5$^+$**–**7$^+$** are nonequivalent. Even at room temperature the methyl groups of **7$^+$** remain non-equivalent, indicative of a large rotational barrier. On the other hand, in the protonated cations **1H$^+$** and **2H$^+$**, we can observe two different isomers only at *ca.* −70 °C (see Fig. 3). By warming the samples, the rotation around the (HO$^+$=C)–C(*ipso*) bond becomes faster and at −20 °C just an averaged conformation is observed. The two rotational isomers (ratio *ca.* 2:1) could not be individually identified and the assignment of the chemical

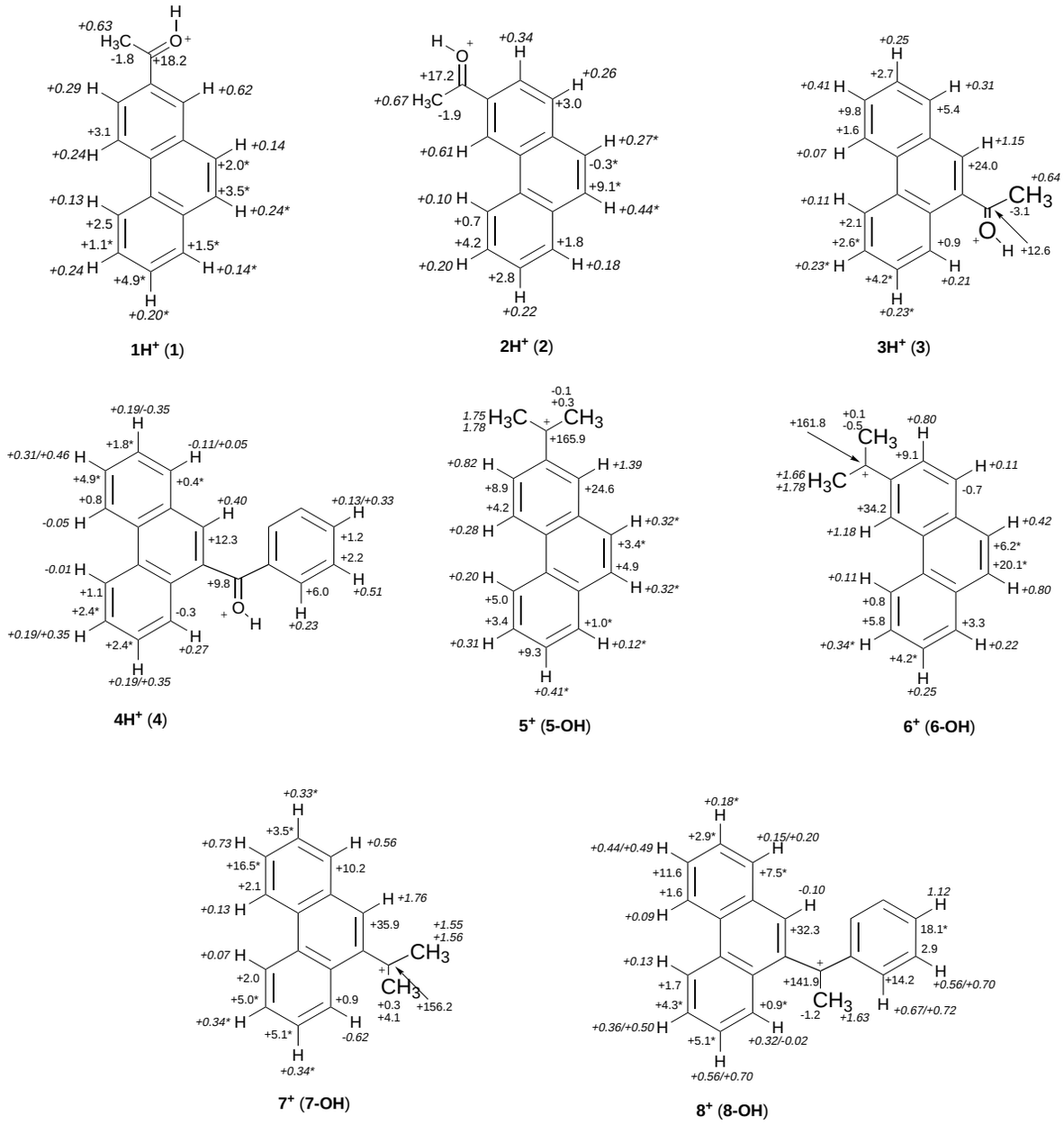

Fig. 3 The $\Delta\delta_C$ and $\Delta\delta_H$ values in the carbocations and carboxonium ions; * means one of the two or both δ values were derived from chemical shifts that were interchangeable (for $\mathbf{4H}^+$ and $\mathbf{8}^+$ double figures refer to max. and min. possible values)

shifts was only possible for the averaged structure at −20 °C. Except for the two *ortho*-carbons which could not be observed (probably due to broadening), all other carbon and proton resonances which were split at lower temperature clearly merged at −20 °C.

In protonated 9-acetyl- and 9-benzoyl-phenanthrene ($\mathbf{3H}^+$ and $\mathbf{4H}^+$) only one of the possible isomers is detected at −70 °C (Scheme 2). This observation confirms the AM1 calculated energies for the two different isomers. The $\Delta H_f°$ values for the non-observed isomers are 1.0–1.5 kcal mol^{-1} higher than the experimentally observed isomer, whereas the energy difference between the two geometrical isomers in the 2- and 3-substituted cations is only *ca*. 0.3 kcal.

syn/*anti* Protonation

Additional splitting of the signals due to a possible *syn* or *anti* protonation of the carbonyl group in the carboxonium ions was not observed, either because the difference in energy between the two isomers is too small or because the exchange is too fast. AM1 calculated relative energies of the two possible isomers (*syn*/*anti* protonation) showed a difference of about 0.1 kcal mol^{-1}.

Structural features in $4H^+$ and 8^+ carbocations

An interesting observation was made by comparing the H-10 proton chemical shifts in the 9-substituted phenanthrene carboxonium ion and carbocation. For $\mathbf{3H}^+$ the H-10 chemical shift is at δ 9.32 whereas in $\mathbf{4H}^+$ this proton is only at δ 8.16. The difference between the H-10 chemical shifts in $\mathbf{7}^+$ (δ 9.58) and $\mathbf{8}^+$ (δ 8.05) is even larger. Its origin is not merely the fact that the phenyl groups in $\mathbf{4H}^+$ and $\mathbf{8}^+$ stabilize more positive charge than the methyl groups do in $\mathbf{3H}^+$ and $\mathbf{7}^+$. The C-10 carbon resonances for example do not show such a big difference ($\mathbf{3H}^+$: δ 154.6; $\mathbf{4H}^+$: δ 141.7; $\mathbf{7}^+$: δ 159.6; $\mathbf{8}^+$: δ 158.0). The unusual proton shielding is apparently due to transannular shielding of the phenyl group. In the AM1-calculated minimized structures for $\mathbf{4H}^+$ and $\mathbf{8}^+$, H-10 is located right above the phenyl group (in both cases). Such transannular effects could explain the 1–1.5 ppm shielding of H-10 in $\mathbf{4H}^+$ and $\mathbf{8}^+$ as compared to the methyl analogs.

Diol epoxide ring opening

Charge delocalization into the phenanthrene system in the model arenium ions and carboxonium ions is most effective from the *meso* position. Based on the magnitude of $\Delta\delta_C$, the

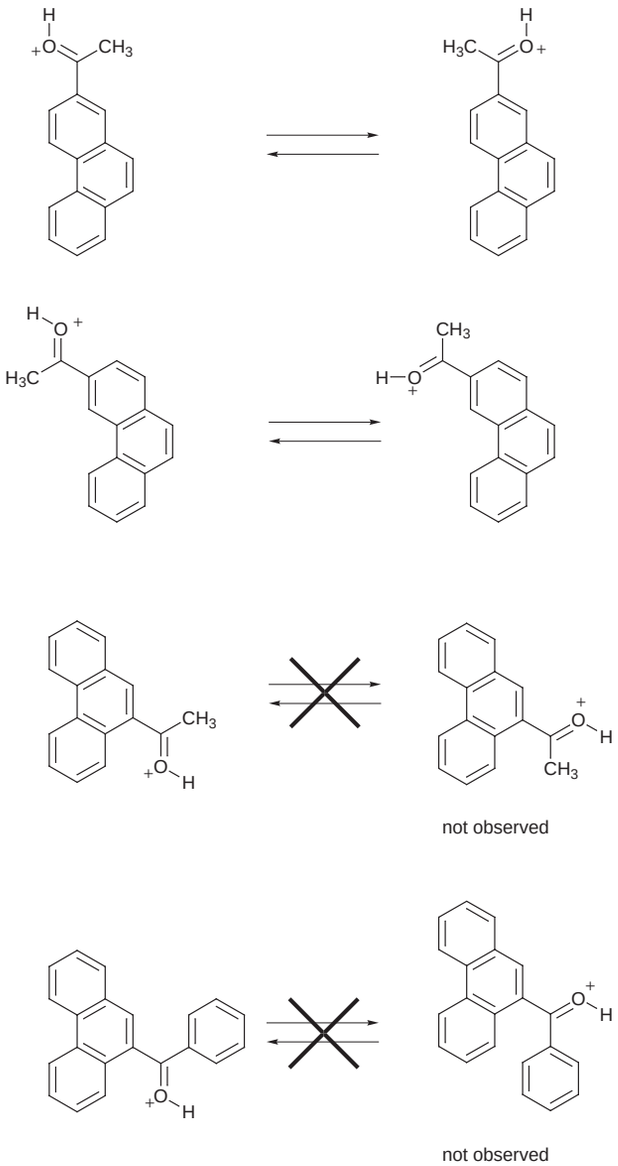

Scheme 2 Rotational isomers

delocalization sequence $\mathbf{7}^+$ ($\mathbf{8}^+$) > $\mathbf{6}^+$ > $\mathbf{5}^+$ can be deduced for the carbocation intermediates, whose involvement in the diol epoxide ring opening process has been inferred based on previous kinetic and solvolytic studies. Since $\mathbf{9}^+$ and $\mathbf{10}^+$ could not be generated and studied for comparison, we resorted to AM1 calculations for a general idea of the relative stabilities based on ΔH_f^0 values: AM1 predicted that $\mathbf{6}^+$ and $\mathbf{5}^+$ should have very close energies (within 1 kcal mol^{-1}) and that $\mathbf{9}^+$ should be more stable than $\mathbf{7}^+$ by *ca*. 2.5 kcal mol^{-1}. Moreover, the corresponding cyclic carbocation $\mathbf{9e}^+$ is predicted to be more stable than $\mathbf{7b}^+$ by *ca*. 1 kcal mol^{-1}. Whereas the predicted charge delocalization pattern for $\mathbf{9}^+$ and $\mathbf{6}^+$ is very similar, the cyclic analog exhibits greater arenium ion character and increased Phen–C^+ bond order (1.39 *vs*. 1.37 Å).

Earlier studies have suggested that methylated PAHs may be converted to PAH–CH_2OH derivatives which are then transformed into esters, which can produce PAH–CH_2^+ carbocations. Carcinogenicity in methylated PAHs appears to correlate with the stability of arylmethyl carbocations, for instance 6-methylbenzo[*a*]pyrene is more potent than BaP.[25] In the present study, based purely on the NMR studies of the persistent model carbocations, the potency order **7a** > **6a** > **5b** may be predicted for the diol epoxides, but taking into account the predicted close relative energies of the carbenium ions in an expanded isomeric set, it may be argued that they can potentially all be important *en route* to PAH–DNA adduct formation and onset of cell damage! Our simple model studies have not taken into account the role of DNA and issues pertaining to DNA base-sequence selectivity, steric/conformational effects and repair. In future work, we hope to draw a biological parallel by examining the DNA-binding ability of the regioisomeric alcohols **5-OH**–**8-OH** in cells in culture.

Experimental

NMR spectroscopy

NMR spectra were recorded on a GE GN-300 wide bore instrument. The NMR spectra of the precursors were recorded at room temperature using $CDCl_3$ as solvent (δ_H 7.26, δ_C 77.0). The cation spectra were obtained at temperatures between −20 and −80 °C; CH_2Cl_2 was used as internal standard (δ_H 5.32, δ_C 53.8). Copies of the C/H HETCOR spectra for the carbocations $\mathbf{7}^+$, $\mathbf{8}^+$, $\mathbf{5}^+$ and $\mathbf{6}^+$, C/H HECTOR spectra for the carboxonium ions $\mathbf{4H}^+$, $\mathbf{1H}^+$ and $\mathbf{2H}^+$ and the H/H COSY and ^{13}C NMR spectra for $\mathbf{3H}^+$ (9 pages) are available as supplementary material (SUPPL. NO. 57362). For details of the Supplementary Publications Scheme see 'Instructions for Authors', *J. Chem. Soc.*, *Perkin Trans. 2*, available *via* the RSC Web page (http://www.rsc.org/authors).

Materials

Phenanthrene, 2-, 3- and 9-acetylphenanthrene **1**–**3**, methyllithium, benzoyl chloride and $AlCl_3$ (all Aldrich) were used without further purification. FSO_3H (Allied) was purified by double distillation at atmospheric pressure under argon. SO_2ClF was prepared by a modified procedure of Reddy *et al.*[26] from SO_2Cl_2, ammonium fluoride and CF_3CO_2H (Aldrich). Several distillation provided pure SO_2ClF.

Synthesis

9-Benzoylphenanthrene 4.† A mixture of benzoyl chloride (3.26 ml, 36 mmol) and $AlCl_3$ (4.29 g, 33 mmol) was heated until a clear solution resulted. The mixture was cooled to room temperature and 24 ml of anhydrous CS_2 was added, followed by phenanthrene (5 g, 28 mmol) which was added slowly over a 20 min period (HCl evolution). After an additional 20 min, the mixture was cooled in an ice bath, the precipitate was collected and decomposed by adding a mixture of ice and 10 M HCl to give a dark brown solid. After extraction with Et_2O (3×) the combined organic layer was washed with saturated aqueous $NaHCO_3$ and ice water, and dried ($MgSO_4$). Evaporation of the solvent resulted in a brown oil which was purified twice by column chromatography [pentane–Et_2O (10 : 1) and hexane–chloroform (10 : 1)] to give 5.4 g of a slightly yellow oil (64%) (for NMR data, see Tables 2 and 4).

General procedure for the synthesis of the alcohols 5-OH–8-OH. The ketones **1**–**4** (*ca*. 0.5–1.5 mmol) were dissolved in anhydrous Et_2O (50–100 ml) under argon. A 5–10-fold excess of methyllithium (*ca*. 1.4 M in Et_2O) was slowly added at room temperature, and the solution was stirred for 2–4 h. The reaction mixture was cooled in an ice bath and 100–200 g of ice was carefully added to the solution. The aqueous layer was extracted three times with Et_2O and the combined organic layer was washed with ice water and ice cold brine, and dried over $MgSO_4$. After evaporation of the solvent, the slightly yellow alcohols **5-OH**–**8-OH** were purified by column chromatography [pentane–Et_2O (5 : 1–2 : 1)] to give the colorless solid products (yields 87–93%) (for NMR data, see Tables 2 and 4).

GC–MS analysis of the alcohols.—GC–MS analysis of **5-OH**–**8-OH** gave in all cases the expected M^+ (*m*/*z* 236). However, the most abundant fragment cation formed in the gas

† The literature procedure (P. H. Gore, *J. Org. Chem.*, 1957, *57*, 135) describes the synthesis of 1-benzoylphenanthrene in 19% yield, but we observed only the 9-substituted isomer.

phase was the hydroxy carbocation $ArC(Me)OH^+$ (*m*/*z* 221), with the relative abundance of $ArC(Me)_2^+$ ions (*m*/*z* 219) being almost negligible.

General procedure for stable ion generation. In a typical experiment, about 30 mg of **1**–**4** or **5-OH**–**8-OH** was placed in a 5 mm NMR tube. The NMR tube was then connected to the high vacuum line (ace-thread port). After several cycles of evacuation and flushing with argon, the NMR tube was evacuated for 5 min. About 0.3 ml of SO_2ClF was then condensed into the NMR tube, which was cooled to liquid nitrogen temperature. After completion of the SO_2ClF addition, the liquid nitrogen bath was exchanged for a dry ice–acetone bath and about 0.05 ml of FSO_3H was carefully added under argon. After vigorous stirring at −78 °C (vortex) the color of the protonated ketone solutions (**1H**$^+$–**4H**$^+$) turned orange–red and the carbocation solutions (**5**$^+$–**8**$^+$) turned deep red. About 0.1 ml of CD_2Cl_2 was slowly added under argon and the cold sample was thoroughly mixed (vortex) to give clear homogeneous solutions.

AM1 calculations

AM1 calculations and energy minimizations were performed with the HYPERCHEM package (HYPERCUBE 1993).

Acknowledgements

Support of our work on reactive intermediates of carcinogenesis of PAHs by the NCI of NIH (R15CA63595) is gratefully acknowledged.

References

1 R. G. Harvey, in *Polynuclear Hydrocarbons and Carcinogenesis*, ed. R. G. Harvey, ACS Symposium Series 283, ACS, Washington DC, 1985, ch. 3; R. G. Harvey, *Polynuclear Aromatic Hydrocarbons: Chemistry and Carcinogenicity*, Cambridge University Press, Cambridge, 1991.
2 W. Levin, A. Wood, R. Chang, D. Ryan, P. Thomas, H. Yagi, D. Thakker, K. Vyas, C. Boyd, S.-Y. Chu, A. Conney and D. Jerina *Drug. Metab. Rev.*, 1982, **13**, 555.
3 M. Koreeda and R. Gopalaswamy, *J. Am. Chem. Soc.*, 1995, **117**, 10 595.
4 R. E. Lehr, M. Singh and C. Utermoehlen, *J. Org. Chem.*, 1987, **52**, 5576.
5 (*a*) A. S. Kiselyov, H. Lee and R. G. Harvey, *J. Org. Chem.*, 1995, **60**, 6123; (*b*) A. S. Kiselyov, T. Steinbrecher and R. G. Harvey, *J. Org. Chem.*, 1995, **60**, 6129.
6 P. P. Fu and R. G. Harvey, *J. Org. Chem.*, 1979, **44**, 3778.
7 P. Y. Bruice, T. C. Bruice, P. M. Dansette, H. G. Selander, H. Yagi and D. M. Jerina, *J. Am. Chem. Soc.*, 1976, **98**, 2965; P. Y. Bruice, T. C. Bruice, H. Yagi and D. M. Jerina, *J. Am. Chem. Soc.*, 1976, **98**, 2973; N. T. Nashed, J. M. Sayer and D. M. Jerina, *J. Am. Chem. Soc.* 1993, **115**, 1723.
8 N. T. Nashed, S. K. Balani, R. J. Loncharich, J. M. Sayer, D. Y. Shipley, R. S. Mohan, D. M. Whalen and D. M. Jerina, *J. Am. Chem. Soc.*, 1991, **113**, 3910.
9 N. T. Nashed, A. Bax, R. J. Loncharich, J. M. Sayer and D. M. Jerina, *J. Am. Chem. Soc.*, 1993, **115**, 1711.
10 N. T. Nashed, T. V. S. Rao and D. M. Jerina, *J. Org. Chem.*, 1993, **58**, 6344.
11 H. Yagi, J. M. Sayer, D. R. Thakker, W. Levin and D. M. Jerina, *J. Am. Chem. Soc.*, 1987, **109**, 838.
12 J. W. Keller, N. G. Kundu and C. Heidelberger, *J. Org. Chem.*, 1976, **41**, 3487.
13 M. D. Hylarides, T. A. Lyle, G. H. Daub and D. L. van der Jagt, *J. Org. Chem.*, 1979, **44**, 4652.
14 D. L. Whalen, N. B. Islam, S. C. Gupta, J. M. Sayer and D. M. Jerina, in *Polynuclear Aromatic Hydrocarbons*, *Measurements*, *Means and Metabolism*, ed. M. Cooke, K. Loening and J. Merritt, Battelle Press, Columbus, 1991, pp. 1021–1035.
15 Review: K. K. Laali, *Chem. Rev.*, 1996, **96**, 1873.
16 K. K. Laali, S. Hollenstein, R. G. Harvey and P. E. Hansen, *J. Org. Chem.*, 1997, **62**, 4023.
17 K. K. Laali, S. Hollenstein and P. E. Hansen, *J. Chem. Soc.*, *Perkin Trans. 2*, 1997, 2207.
18 K. K. Laali and P. E. Hansen, *J. Org. Chem.*, 1997, **62**, 5804.
19 K. K. Laali, M. Tanaka, S. Hollenstein and M. Cheng, *J. Org. Chem.*, 1997, **62**, 7752.
20 *Reviews:* (*a*) M. Rabinovitz and Y. Cohen, *Tetrahedron*, 1988, **44**, 6944; (*b*) M. Rabinovitz, *Top. Curr. Chem.*, 1988, **148**, 99; (*c*) K. Mullen, *Chem. Rev.*, 1984, **84**, 603.
21 (*a*) Y. Cohen, J. Klein and M. Rabinovitz, *J. Am. Chem. Soc.*, 1988, **110**, 4634; (*b*) K. Mullen, T. Meul, P. Schade, H. Schmickler and E. Vogel, *J. Am. Chem. Soc.*, 1987, **109**, 4992; (*c*) B. Eliasson, D. Johnels, I. Sethson and U. Edlund, *J. Chem. Soc.*, *Perkin. Trans. 2*, 1990, 897.
22 D. R. Boyd, N. D. Sharma, S. K. Agrawal, G. S. Gadaginamath, G. A. O'Keane, W. B. Jennings, H. Yagi and D. M. Jerina, *J. Chem. Soc.*, *Perkin Trans. 1*, 1993, 423.
23 (*a*) M. Rabinovitz and A. Ayalon, *Pure Appl. Chem.*, 1993, **65**, 111; (*b*) L. Zelikovich, R. E. Hoffman, A. Ayalon and M. Rabinovitz, *J. Chem. Soc.*, *Perkin Trans. 2*, 1992, 1785.
24 (*a*) J. R. Rabinowitz and S. B. Little, *Int. J. Quantum Chem.*, 1994, **52**, 681; (*b*) J. R. Rabinowitz and S. B. Little, *Chem. Res. Toxicol.*, 1992, **5**, 286.
25 R. E. Royer, T. A. Lyle, G. G. Moy, G. H. Daub and D. L. Vander Jagt, *J. Org. Chem.*, 1979, **44**, 3202.
26 P. V. Reddy, D. R. Bellew and G. K. S. Prakash, *J. Fluorine Chem.*, 1992, **56**, 195.

Paper 7/07423I
Received 14*th October* 1997
Accepted 30*th January* 1998